Faster *Cryptococcus* melanization increases virulence in experimental and human cryptococcosis

Herdson Renney de Sousa[1], Getúlio Pereira de Oliveira Júnior[2], Stefânia de Oliveira Frazão[3], Kaio Cesar de Melo Gorgonha[1], Camila Pereira Rosa[1], Emãnuella Melgaço Garcez[1], Joaquim Lucas Junior[4], Amabel Fernandes Correia[5], Waleriano Ferreira de Freitas[1], Higor Matos Borges[1], Hugo Costa Paes[1], Luciana Trilles[6], Marcia dos Santos Lazera[6], Vitor Laerte Pinto Junior[4], Maria Sueli Soares Felipe[7], Arturo Casadevall[8], Ildinete Silva-Pereira[3], Patrícia Albuquerque[3,9], André Moraes Nicola[1,7,*].

[1]Faculty of Medicine, University of Brasília, Brasília, DF, Brazil.

[2]Division of Allergy and Inflammation, Department of Medicine, Beth Israel Deaconess Medical Center, Harvard Medical School, Boston, MA, United States.

[3]Laboratory of Molecular Biology of Pathogenic Fungi, Institute of Biological Sciences, University of Brasília, Brasília, DF, Brazil.

[4]Oswaldo Cruz Foundation (Fiocruz – Brasília), Brasília, DF, Brazil.

[5]Central Public Health Laboratory (Lacen-DF), Brasília, DF, Brazil.

[6]Mycology Laboratory, Evandro Chagas National Institute of Infectious Diseases, Oswaldo Cruz Foundation (Fiocruz – Rio de Janeiro), Rio de Janeiro, RJ, Brazil

[7]Graduate Program in Genomic Sciences and Biotechnology, Catholic University of Brasília, Brasília, DF, Brazil.

[8]Department of Molecular Microbiology and Immunology, Johns Hopkins Bloomberg School of Public Health, Baltimore, MD, USA.

[9]Faculty of Ceilândia, University of Brasília, Brasília, DF, Brazil.

Corresponding author:
Name: André Moraes Nicola
Address: Campus Universitário Darcy Ribeiro, Núcleo de Medicina Tropical, sala 40. Brasília-DF, Brazil. 70910-900.
Phone: +55 61 992619048
E-mail: amnicola@unb.br

Conflict of interest statement: The authors have declared that no conflict of interest exists.

31 **Graphical abstract**

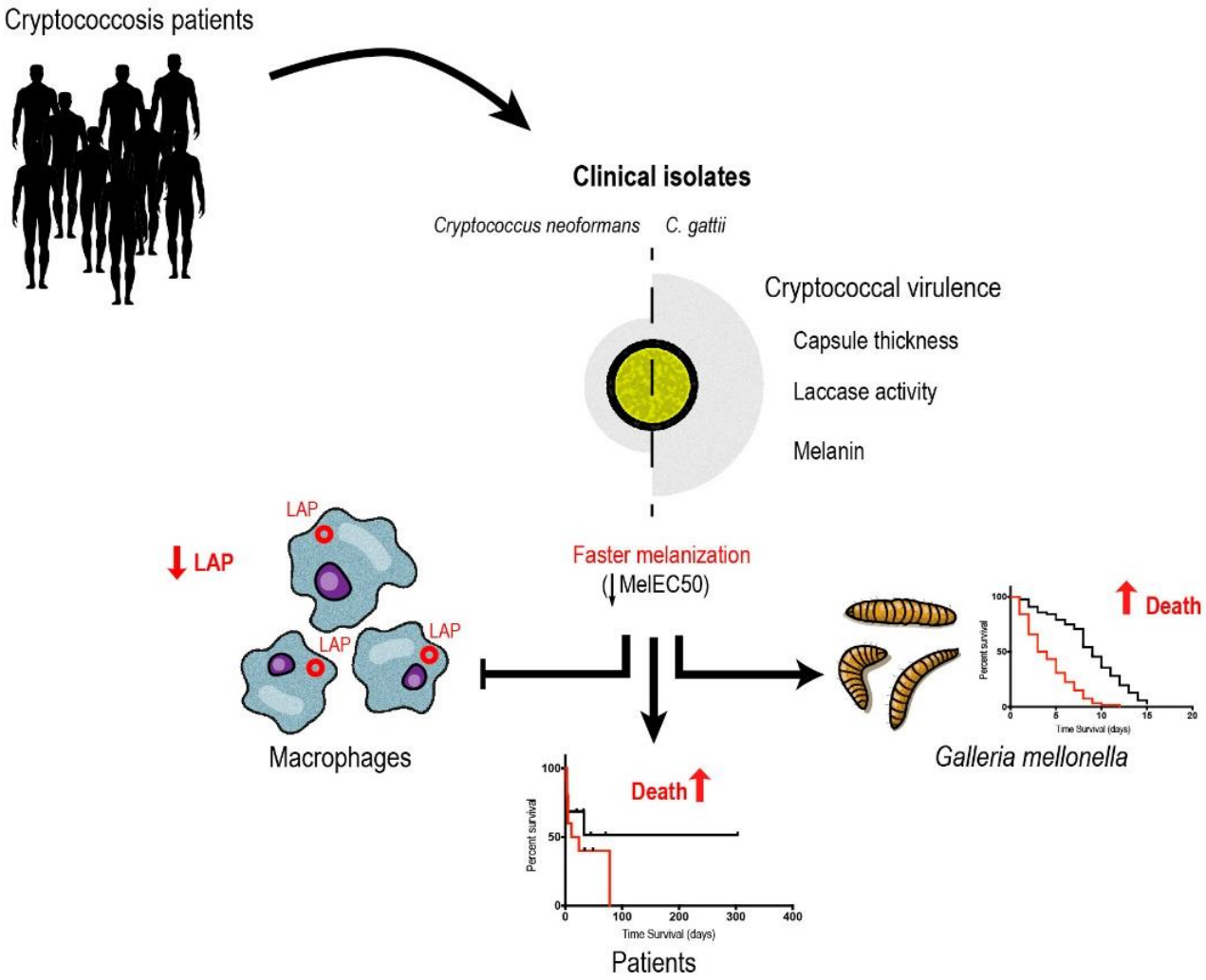

32

33

Abstract

Cryptococcus spp. are important human pathogens responsible for about 180,000 deaths per year. Studying their virulence attributes can lead to better cryptococcosis prevention and treatment. In this work, we systematically investigated virulence attributes of *Cryptococcus* spp. clinical isolates and correlated them with patient data. We collected 66 *C. neoformans* and 19 *C. gattii* isolates from Brazilian patients and analyzed multiple phenotypes related with their capsule, production of laccase, melanin and extracellular vesicles. We also tested their virulence in *Galleria mellonella* and ability to evade macrophage LC3-associated phagocytosis (LAP). All phenotypes analyzed varied widely among the isolates, but *C. neoformans* isolates tended to melanize faster and more intensely and produce thinner capsules in comparison with *C. gattii*. We also observed correlations that match previous studies, such as that between secreted laccase – but not total melanin production – and disease outcome in patients. The most striking results, though, came from our measurements of *Cryptococcus* colony melanization kinetics, which followed a sigmoidal curve for most isolates. Faster melanization correlated positively with LAP evasion, virulence in *G. mellonella* and worse prognosis in humans. These results suggest that the speed of melanization, more than the total amount of melanin *Cryptococcus* spp. produces, is crucial for virulence.

Introduction

Cryptococcosis is estimated to cause 181.000 deaths per year, mostly in low and middle-income countries (1). Infection occurs through inhalation of spores or desiccated yeast cells of the species complexes *Cryptococcus neoformans* or *C. gattii*. In most cases, the disease happens in hosts with defective immunity secondary to AIDS, cancer or medication (2). The association of Amphotericin B and flucytosine is the gold standard treatment (3), but even in high income countries the case fatality rates are around 20%. In regions where these drugs are not available and fluconazole is the only choice, the case fatality rates can be higher than 60% (1). Combined with the fact that there are no vaccines, there is a clear need for more effective preventative and therapeutic options.

C. neoformans and *C. gattii* have several well-studied virulence factors such as the ability to produce melanin (4), the presence of a polysaccharide capsule (5), the ability to grow at 37 °C and the secretion of urease and other extracellular enzymes (6). Of these, the capsule and melanin contribute almost half of the *C. neoformans* virulence (7). The cryptococcal capsule is composed mainly of polysaccharides, such as glucuronoxylomannan (GXM). Its presence and thickness interfere with macrophage phagocytosis, and capsular polysaccharides interfere with the activation and differentiation of T cells (5, 8). Studies in mice and translational studies with cryptococcosis patient samples have shown the importance of GXM secretion by *C. neoformans* on central nervous system infections by *C. neoformans* (9, 10).

Melanin is a brown or black, hydrophobic, high molecular weight, negatively charged pigment. It is present in the cryptococcal cell wall and protects the yeast cell against host and environmental stresses (11). The pigment also increases resistance to Amphotericin B and affects susceptibility to fluconazole (12). In pathogenic species of the genus *Cryptococcus*, melanin production is dependent on laccase enzymatic action on biphenolic compounds (13). A translational

study with *C. neoformans* clinical isolates demonstrated that laccase also has other roles that are crucial for fungal survival in the cerebrospinal fluid, and that isolates with more effective melanin-independent secreted laccase roles were associated with poorer patient outcomes (14).

Given that several tools presently used to prevent and treat infectious diseases target microbial virulence factors, we delved further into the roles played by capsule, melanin, laccase and extracellular vesicles in the interaction between *Cryptococcus* spp. and their host. The strategy consisted of collecting clinical isolates and patient data, characterizing the isolates in the laboratory and correlating the experimental results with patient outcomes. We found several correlations that confirm previous observations, but also important correlations between the melanization kinetics and outcomes of the interaction between *Cryptococcus* spp. and macrophages or *G. mellonella*. Most importantly, we also found that faster melanization, but not the final amount of melanin on cryptococcal colonies, correlated with the survival of HIV-positive patients with severe cryptococcosis. These findings help us better understand the mechanisms used by *Cryptococcus* spp. to survive and cause disease in their hosts.

Results

Clinical and epidemiological data

Cryptococcus spp. clinical isolates analyzed in this study are from two different sources. Twenty-eight (16 *C. neoformans* and 12 *C. gattii*) are from a cohort of patients treated in Rio de Janeiro, Brazil, about whom we have no clinical information. The second group of clinical isolates are from an ongoing epidemiological study in Brasília, Brazil. It contains 54 isolates (7 *C. gattii* and 47 *C. neoformans*) from 41 patients. From these, 37 were from the cerebrospinal fluid (CSF), 1 from a blood culture, 1 from a tissue biopsy and 2 from bronchoalveolar lavage fluid. Thirty-seven patients were infected by *C. neoformans* only, 2 by *C. gattii* only and the other 2 had *C. neoformans*/*C. gattii* mixed infections. Available information about them and the patients from which they were isolated can be found in Table S1.

All patients from the Brasília study (Table 1) were diagnosed and treated in public hospitals, according to the standards used by the services in which they were assisted. Most were male (68.3%), and their mean age was 42 years. HIV infection was reported in 68.3%; of the 12 HIV-negative patients, two had diabetes, three were using corticosteroids, one was using corticosteroids plus a second immunosuppressive drug, one had a primary immunodeficiency and eight had no known risk factor. Among the 39 patients that we were able to follow until death or hospital discharge, the 2-week and 10-week mortality rates were respectively 30.8% and 41%.

Melanization kinetics

The method we used to measure melanin production by each isolate quantitatively was based on a previously published protocol (15) (Figure S1A). To do so, we spotted a specific number of fungal cells in 24-well plates filled with solid medium containing the melanin precursor L-DOPA. These plates were photographed at regular intervals during incubation, and the resulting digital

images processed to quantify how dark the colonies had become at each point in time. For most isolates, the resulting data fit very well in a sigmoidal curve. This method was highly reproducible, as shown by the similarity between the curves obtained from five independent experiments performed in different days with the control strain H99 (Figure S1B). As shown in Figures S1C-D, some isolates, such as H99, melanized faster and became black at the end of the experiment, whereas others, such as CNB017.1, melanized slowly and never became black. We also found differences in the pattern of colony melanization, such that some isolates (e.g. H99 and CNB017.1) showed homogeneously pigmented colonies whereas others had more intense melanization either in the periphery (CNB013.1) or in the center (CGF007) of the colony.

Using logistic regression, we quantitatively evaluated the kinetics of melanin production by each isolate. This regression resulted in five melanization parameters, three of which with a specific biological meaning:

- Bottom – median gray level of the colony at the first time point.
- Top – median gray level of the colony at the end of the experiment. Indicates how dark the colony becomes, and thus the final amount of melanin it produces.
- Span: Top minus Bottom.
- Hill Slope: steepness of the curve. Indicates how fast the colony produces melanin during the time in which melanization is occurring.
- EC50: Time it takes for the colony to reach half of its final melanization intensity. Measures both how soon the colony starts melanizing and how fast it produces melanin once it has started.

A great variety was observed in the melanization parameters between isolates (Figure 1A-C), except for the melanization slope, which has a less dispersed frequency distribution (Figure 1D). To validate this new methodology, we compared its results with a semi-quantitative analysis we had

previously done of 16 clinical isolates (Figure S2A). These isolates were grown in solid melanin-inducing medium and photographed every 12 h for 7 days. After cropping all photos of each colony together, we visually ranked them based on how fast they melanized and how dark they eventually became. The isolates were then given a score of 1 to 7: 1 for those with slowest melanization and less dark colonies and 7 for those with the highest rate of colony pigmentation. We found a significant correlation between this visual score and the logistic regression parameter Top (Figure S2B), indicating that our image analysis method matches the visual ranking. As expected, the visual melanization score also correlated directly with Span ($r = 0.456$) and Hill Slope ($r = 0.226$) and inversely with EC50 ($r = -0.254$), but these correlations were not statistically significant (p-values of 0.066, 0.379 and 0.321, respectively).

In addition to melanization, we also measured laccase activity both on washed whole cells ($n= 84$) and on the culture supernatants ($n = 82$). We observed greater dispersion in the frequency distribution of secreted laccase activity (Figure 1E) than whole-cell laccase activity (Figure 1F). Interestingly, the laccase activity in culture supernatants, but not on whole cells, correlated well with the visual melanization score (Figure S2C) and melanization EC50 (Figure S2D).

Clinical isolates demonstrate the variation of secreted GXM and capsule size in different culture media

To evaluate the capsule from each clinical isolate, we grew them in different media, photographed the cells with India ink and measured their capsule thickness. The media we used included Sabouraud, a rich medium in which the cryptococcal capsule is not induced, and three capsule inducing media: Sabouraud diluted 1:10 with MOPS pH 7.5 (Sab-MOPS), minimum medium (MM) and CO_2-independent medium (CIM). The baseline capsule thickness in non-inducing medium varied from 0.5 to 5 μm for different isolates, although more than 90% of the clinical isolates had capsules 1

156 to 2 µm thick (Figure 2A). Representative pictures of clinical isolates at both extremes variation of
157 capsule thickness is shown in Figure 2B. To determine the capacity for capsule induction, we measured
158 the capsules for each isolate in each inducing medium and divided the value by that obtained in
159 Sabouraud (Figure 2C-F). Sab-MOPS medium resulted in the greatest capsule induction, the most
160 notable of which that of CNF016 (Figure 2 D). However, even in this medium some isolates such as
161 CGB009.1 maintained a capsule thickness that was very similar to that in Sabouraud, indicating that
162 different isolates may respond differently to the signals that induce capsule.

163 As capsular polysaccharides can be secreted in soluble form, we also used a capture ELISA to
164 determine the concentrations of GXM on the culture supernatants of the clinical isolates. As observed
165 with other virulence factors, the values we obtained varied widely across clinical isolates (Figure 2G).

166 **Clinical isolates present different profiles of interaction with macrophages**

167 Macrophages are crucial effector cells in the immune response to *Cryptococcus* spp. A specific
168 type of autophagy, LC3 associated-phagocytosis (LAP), is important for the fungicidal activity of
169 macrophages (16). As previous studies with *Aspergillus fumigatus* showed that melanin inhibited LAP
170 (17, 18), which is important in immunity against *C. neoformans* (19), we quantified LAP in
171 macrophage-like J774 cells infected with antibody-opsonized clinical isolates.

172 The infected J774 cells were processed for LC3 immunofluorescence microscopy and imaged.
173 For each isolate, we evaluated the images to calculate two variables: the proportion of macrophages
174 with LC3 recruitment to at least one phagosome containing *C. neoformans* and the proportion of
175 macrophages where all internalized fungi were on LC3-positive phagosomes. Figure 3A shows
176 representative immunofluorescence images with the two isolates that had the lowest (CNB020) and the
177 highest (CNB042) proportion of LC3-positive phagosomes. In none of the isolates tested all

internalized fungi were noticed in LC3-positive phagosomes (Figure 3B), possibly indicating that *Cryptococcus* spp. has mechanisms to avoid this type of macrophage response.

***C gattii* isolates have larger capsules and more secreted laccase activity, but *C. neoformans* melanizes faster and more intensely**

After systematically measuring virulence and host-pathogen interaction attributes, we began mining them for important insights into cryptococcal virulence. We observed important differences in the expression of virulence factors between *C. neoformans* and *C. gattii*. A larger proportion of *C. neoformans* isolates (23 out of 57) had a homogeneous colony melanization pattern, in comparison with just one out of 19 *C. gattii* isolates ($p = 0.004$, Fisher's exact test). *C. neoformans* isolates also melanized faster (lower melanization EC50) and accumulated more melanin at the end of the experiment (higher melanization Top), with no differences on Hill Slope and Span (Figure 4 A-D). The two species also differed in laccase activity, with more secreted laccase activity in the supernatants – but not whole cells – of *C. gattii* isolates (Figure 4 E-F).

C gattii isolates had thicker capsules than *C. neoformans* in non-inducing Sabouraud medium (Figure 4G). *C gattii* isolates also induced their capsules to a larger extent than *C. neoformans* in all capsule-inducing media, with the differences being statistically significant in all but minimal medium (Figure 4H-J). The slightly higher amount of GXM secreted into the supernatant of *C. gattii* cultures was not significant ($p = 0.319$, two-tailed t-test) (data not shown).

The amount of secreted extracellular vesicles correlates with capsule thickness, melanization and secreted laccase activity

Given that extracellular vesicles (EVs) are necessary for the export of capsular polysaccharides and laccase (20, 21), we also studied the EVs isolated from a subset of *C. neoformans* isolates. We used an indirect method to quantify them, measuring the concentration of

ergosterol in cell-free supernatants (22) and dividing this by the number of cells (Figure 5A). Besides, we also measured the hydrodynamic diameters and polydispersity indices of the vesicle preparations by dynamic light scattering (DLS) (Figure 5B-C). We observed significant correlations between EV-ergosterol content and the visual melanization score and melanization EC50 (Figure 5D-E), but not with melanization Top and Span (Figure 5F-G). EV-ergosterol also showed significant correlation with whole-cell laccase activity and secreted laccase activity (Figure 5H-I). The indirect EV measurement in the supernatants of clinical isolates also correlated well with their basal capsule thickness in Sabouraud, but not with their ability to induce capsule in any of the three tested media (Figure 5J-N).

Melanization kinetics of clinical isolates affect the ability to escape from LC3- associated phagocytosis in macrophages

We correlated the LAP proportions described above with melanin and capsule phenotypes. The proportion of macrophages with LC3-positive phagosomes correlated strongly with melanization EC50 and inversely with melanization Top and Span (Figure 6A-C), but not with secreted laccase activity (Figure 6D). In contrast, no significant correlation between the proportion of macrophages with LC3-positive phagosomes and any of the capsule variables was found (Figure S3).

Melanization kinetics, laccase activity and the capsule of clinical isolates affect survival in *G. mellonella*

We infected wax moth (*G. mellonella*) larvae with the clinical isolates to evaluate the role of melanization, laccase activity and capsule on virulence. This experiment was made with 15 *C. gattii* and 31 *C. neoformans* isolates divided into three lots. The survival curves for one of these lots is shown as an example in Figure 7A, whereas the distribution of median *G. mellonella* larvae survival times is shown in Figure 7B.

Using Cox proportional hazards regression, a multivariate survival tool, we generated a statistical model which evaluated the impact of virulence phenotypes upon survival time for all infected larvae (n = 588). In addition to virulence variables, we added as possible confounding variables the *Cryptococcus* species of the isolate and diet fed to *G. mellonella* larvae used for infections. The Cox regression model ($X^2 = 258.9$, df = 10, $p < 0.001$) showed significant impacts on *G. mellonella* survival of capsule induction in Sab-MOPS (HR 1.7, 95% CI 1.2–2.4, P = 0.003), melanization EC50 (HR 0.8, 95% CI 0.7–0.9, P = 0.02), melanization Top (HR 2.9, 95% CI 1.6–5.2, P < 0.001), secreted laccase activity (HR 2.6, 95% CI 2.0–3.3, P < 0.001) and the confounding co-variable cereal diet (HR 7.5, 95% CI 5.0–11.2, P < 0.001). Variables that were not significant on this Cox regression model are capsule thickness in Sabouraud, capsule induction in MM and CIM, whole-cell laccase activity and species of *Cryptococcus*.

Secreted laccase activity and melanization EC50 increases the risk of death in patients with disseminated cryptococcosis

To study the impact of these phenotypes on the human disease, we used survival data from patients of the Brasília study for a Cox proportional hazards regression. Of the 41 patients, we included in the regression model only those with systemic disease caused by *C. neoformans* or mixed *C. neoformans*/C. *gattii* (n = 34). Eight patients were HIV negative and 23 HIV positive. The maximum follow-up time was 303 days. Patients who died during the follow-up time were accounted as events (n = 19), whereas the other ones were released after treatment (n = 14) or lost to follow up while still alive (n = 1). The Cox regression model ($X^2 = 13.7$, df = 6, p = 0.032) showed significant impacts on patient survival of the melanization EC50 (HR 0.23, 95% CI 0.06–0.83, P = 0.025) and secreted laccase activity (HR 5.07, 95% CI 1.22–21.09, P = 0.025). Covariates that were not significant on the Cox regression model were age at the time of diagnosis, HIV status, whole-cell laccase activity and melanization Top.

Discussion

Capsule and melanin are two of the most important and studied virulence factors in the *Cryptococcus* genus, allowing the fungal cells to subvert host immunity and cause cryptococcosis. Most studies on these virulence factors are made either in vitro or in animal models, which are both highly informative but not completely applicable to human disease. We used a translational approach to study virulence phenotypes in clinical isolates, their interaction with experimental hosts and finally to associate them with the outcome of the disease in the patients from whom the isolates were obtained. We were thus able to obtain novel information on the role these two virulence attributes play in the pathogenesis of cryptococcal disease.

The most striking observations were related to melanin, a pigment that protects cryptococcal cells against oxidative stress, extreme temperatures and UV radiation (23–27). All isolates tested were able to produce the pigment, although some produced it faster than others and appeared darker at the end of the experiment. This melanization speed correlated negatively with the survival of cryptococcosis patients, suggesting a poor prognosis in infections caused by fast melanin forming strains. Sabiiti and colleagues (14) have previously shown that the amount of secreted laccase correlated well with cryptococcal survival in the cerebrospinal fluid and patient outcome, but when they analyzed the amount of melanin made, they were unable to establish a statistically significant correlation at the $p = 0.05$ level, which was possibly at Type II error. What they measured, however, was the total amount of melanin in the cells of a subset of ten clinical isolates, which might be similar to the Melanization Top variable we measured. Our observations suggest that the melanization speed, rather than the final amount of melanin, could be more important in determining the outcome of human cryptococcosis. This observation makes sense given that melanization protects cells against immune mechanisms and cells that melanize earlier would have a survival advantage.

Because laccase synthesizes melanin, melanization parameters are expected to depend to some extent on laccase production, which means that teasing their roles on outcomes of infection apart can be challenging. However, the present study suggests these roles are at least partly independent. Specifically, figure S2D shows that while laccase secretion generally correlates with melanization speed, outliers do exist that either secrete relatively large amounts of the enzyme, but melanize slowly, and melanize fast while secreting relatively low amounts of the enzyme. Differences in the efficiency of melanin anchoring in the cell wall, in the proportion of free and cell wall-associated laccase, or in the proportion of chitin in the cell wall (the polymer to which melanin is anchored (28)) may perturb the correlation between the two measurements. Statistically, residual plots of our correlation data are symmetric around zero for both variables, which also suggests the assumptions of our model are correct. Moreover, laccase has well-documented effects in infection outcomes that are melanin-independent, such as detoxification of iron (29), prostaglandin production (30) and neutralization of the fungicidal properties of cerebrospinal fluid (14).

Extracellular vesicles (EVs) are associated with several biological roles (31). In fungi, especially *Cryptococcus*, they are associated with the transport of various important virulence molecules like melanin, laccase, nucleic acids and others (20, 21). A *C. neoformans* mutant with impaired EV secretion, obtained through silencing of the *SEC6* gene, presented a decrease in secreted laccase activity and was hypovirulent in mice (20). The formation of capsule and melanin are dependent on the secretion of EVs (32, 33). Hence, we quantified the association between EVs and the phenotypes of the capsule, laccase and melanin of a subset of the isolates, all of the same species of *C. neoformans* and molecular type VNI. The amount of EVs secreted in minimal medium had a strong correlation with laccase activity. Interestingly, we also found that the amount of EVs are associated with faster melanization and the larger capsule thickness in rich medium. On the other hand, we found no correlation with the total amount of melanin, the total amount of secreted GXM or

295 the thickness of the capsule in nutrient-deficient inducing media. These findings highlight the role of
296 EVs in the expression of *C. neoformans* virulence factors. Taken together, our data indicate that
297 factors other than the amount of EVs are important for inducing capsule in nutrient-deficient media.

298 Melanization phenotypes and laccase activity are associated with greater virulence of clinical
299 *Cryptococcus* spp. Isolates (8, 14, 34–38). Genetic and environmental factors contribute to the
300 variation in the melanin production of *C. neoformans* (39, 40), which is under complex cellular
301 regulation (40, 41). Furthermore, the experimental quantification of the pigment presents significant
302 methodological challenges (42). *C. neoformans* showed better melanization capacity compared to *C.*
303 *gattii*. But interestingly, *C. gattii* showed a greater capsule thickness in all media, except for minimal
304 medium (which mimics the environment of cryptococcal meningitis infection, the main manifestation
305 in most severe cases of cryptococcosis). We found that isolates with higher basal capsule thickness
306 (Sabouraud) had a significant correlation with isolates with lower melanization speed (high
307 melanization EC50), but this melanization index did not correlate with capsule thickness in MM. We
308 found significant correlations between secreted laccase activity and relative capsule thickness in Sab-
309 MOPS /Sabouraud medium after 24h of culture. Overall, these data suggest that melanization
310 kinetics, secreted laccase activity and capsule thickness have different expression mechanisms
311 between species. In addition, laccase activity differs not only between species but also at the cellular
312 location where it is quantified. Perhaps higher melanin production and lower capsule thickness are
313 important factors that favor the dissemination and survival of *C. neoformans* in the central nervous
314 system, unlike *C. gattii*, which is strongly associated with pulmonary cryptococcosis (43).

315 The evolutionary divergence of proteins and signaling cascade configurations between *C.*
316 *neoformans* and *C. gattii* may explain the differences in the expression of virulence factors. For
317 example, TPS1 and TPS2 genes were found to be critical for thermotolerance, pathogenicity, capsule
318 and melanin production in *C. gattii* (44), but the homologous genes in *C. neoformans* were required

only for thermotolerance, not for capsule or melanin production (45). This may indicate that the expression of the capsule is influenced not only by the yeast environment, but also by different genetic traits between the two species (10). Here we hypothesize that *C. gattii* ability to infect immunocompetent individuals can be partly explained by the increased basal expression of important virulence factors such as the polysaccharide capsule.

Macrophages are crucial effector cells against fungi. However, some facultative intracellular pathogens, like *Cryptococcus* spp., can survive and replicate inside macrophages. These cells trigger autophagy as part of their response to intracellular pathogens (46, 47). The presence of LC3 (microtubule-associated protein 1 light chain 3 alpha) is associated with autophagosome maturation (48). The autophagy route called LC3 associated-phagocytosis (LAP) is important for the fungicidal activity of macrophages (16). Fungal virulence factors, such as melanin in *Aspergillus fumigatus*, inhibited LAP and increased virulence, *in vitro* and in a murine model (17, 18). In a subset of the clinical isolates, we observed a strong correlation between the melanization kinetics and the inhibition of LAP in murine macrophages.

Wax moth larvae (Lepidoptera) are an invertebrate animal model extensively used for *in vivo* studies of *Cryptococcus* virulence, host innate immunity after infection and the activity of antifungal compounds (49–51). Bouklas and collaborators showed that intracellular phagocytosis, killing by murine macrophages, capsule thickness and laccase activity did not correlate with *C. neoformans* virulence in *G. mellonella*. They found high-uptake strains to have significantly increased laccase activity, and virulence in mice, but not in *G. mellonella* (52). It should be added that methodological differences might explain the discrepancy in observations: Bouklas *et al.* measured laccase activity by melanin accumulation in a liquid culture over 16 hours at 37 °C, plus 24 hours at 25 °C, which corresponds roughly to the whole-cell laccase activity quantitation protocol we used, whereas we measured secreted laccase separately. In other words, there is no disagreement between our data and

343 theirs, since in our work whole-cell laccase also had no detectable influence on the outcome of
344 *Galleria* infection. Another study found that *C. gattii* strains exhibited similar virulence between
345 murine inhalation models and *G. mellonella* infection (53). Following evidence of a deterministic
346 system in *G. mellonella* cryptococcal infection (54), our results support the idea that virulence is an
347 emerging property that cannot be easily predicted by a reductionistic approach, but can be partially
348 resolved by the multivariate regression model. Furthermore, our result is in agreement with a
349 previous report (51) that melanin synthesis was directly related with the level of virulence of four
350 major molecular types of *C. gattii* in *G. mellonella*.

351 In summary, our study showed that melanization kinetics, secreted laccase activity and capsule
352 growth in different inducing media are each associated with the virulence of clinical *Cryptococcus*
353 strains in an invertebrate animal model. EVs, laccase secretion and melanin production represent a
354 continuum that seems to exert the major influence on infection outcomes. A limitation of this study is
355 that our patients were treated with different regimens in distinct health services. In our cohort of
356 patients, faster colony pigmentation together with secreted laccase activity had a significant
357 association with mortality attributed to disseminated cryptococcosis. The clinical isolates *C.*
358 *neoformans* CNB004.1, CNB007.1 and CNB020 presented the lowest MelEC50 values of (faster
359 melanization). Accordingly, they were found to be highly virulent in that the patients that harbored
360 them all died within 25 days after diagnosis with cryptococcal meningoencephalitis. Altogether, we
361 have seen strong correlations and trends, and although this does not necessarily imply causality, the
362 strength and pattern of the associations indicate that melanization kinetics plays a key role in
363 cryptococcal disease. These findings highlight the importance of the role of the laccase-dependent
364 melanin pathway and its relevance to the human clinical outcomes, which suggests the EV-laccase-
365 melanin nexus as an important source of targets for future therapeutic approaches to disseminated
366 cryptococcosis.

Methods

Patients and *Cryptococcus* spp isolates

The isolates used in the study were obtained from two different sources in Brazil. One set came from the Culture Collection of Pathogenic Fungi at Fiocruz, in the city of Rio de Janeiro. The other one from an ongoing epidemiological study in the city Brasília. This study was approved by the Ethics Committee of the Foundation for Teaching and Research in Health Sciences (CEP-FEPECS). Patients or their legal guardians gave written informed consent for the collection of clinical data and specimens, including those from which fungal isolates were obtained.

A total of 82 clinical isolates were used. We added two control strains (H99 and B3501). The 28 isolates from Rio de Janeiro had been previously typed by MLST as *C. neoformans* molecular type VNI and *C. gattii* molecular type VGII, whereas the isolates from Brasília were typed by Sanger-sequencing an URA5 amplicon and comparing the sequence to that of standard strains. With this analysis, 65 isolates were determined to belong to the *C. neoformans* species complex, molecular type VNI, and 19 were typed as belonging to the *C. gattii* species complex, molecular type VGII. We were able to obtain clinical information from the medical records of 41 patients, which are shown in Table 1.

Cryptococcus culture

All yeasts were kept frozen in 35% glycerol on a -80°C freezer. From this stock, the isolates were streaked onto Sabouraud agar medium (2% dextrose, 1% peptone, 1.5% agar, pH 5.5) and grown for 72 hours at 30 °C. Isolated colonies were incubated for 72 hours in Sabouraud-dextrose (Sab) liquid medium (4% dextrose, 1% peptone, pH 5.5; Sigma-Aldrich) at 37°C with 250 rpm shaker rotation. Laboratory reference strains H99 (*C. neoformans* var. grubii, serotype A) and B3501 (*C. neoformans* var. neoformans, serotype D) were used as controls.

Melanin production evaluation

The minimal medium (MM) (15 mM d-Glucose, 10 mM $MgSO_4$, 29.4 mM KH_2PO_4, 13 mM glycine, 3 μM thiamine-HCl) (26) was used in these experiments. The 2X concentrated MM and 3% agar were prepared separately. As thiamine and L-DOPA can be degraded at high temperatures, the agar was heated separately and, after reaching the temperature of 60°C, was mixed with the 2X MM, reaching a final concentration of 1.5% agar and 1X MM. After that, the medium was supplemented with 1 mM L-DOPA (Sigma-Aldrich). Then 1 mL of the MM agar was added to each well in a 12 well plate protected from light. In the center of each well, 5 μL of each isolate containing a total of 10^5 cells were inoculated. All inocula were made in duplicates, in two different wells. The plates were incubated at 37 °C protected from light and monitored for 7 days. After 24 hours of incubation, we photographed each plate every 12 hours. The photographs were taken inside a biosafety cabinet, using a mirror apparatus specially prepared to photograph culture plates. With these conditions, it was possible to standardize the illumination and photography parameters during the capture of all images. A Nikon D90 digital single-lens reflex (D-SLR) camera equipped with and 85 mm lens was used, with fixed focal length, exposure time, ISO setting, aperture, and white balance. The colony melanization phenotype was also evaluated and classified into heterogeneous (melanization mostly at the center or edges of the colony) or homogeneous colony melanization.

Semi-quantitative melanization score

Based on the images collected as described above, the isolates were qualitatively categorized into 7 groups ordered from 1 to 7. Group 1 contains the colony with less intense and slower melanization and group 7 the isolates with more intense and faster melanin production. Each isolate was scored independently by two researchers that were blinded to each other's evaluation, and the outcomes were very similar.

Melanin quantification in grayscale

We also created a protocol based on previous publications (15, 55) to quantitatively analyze the images described above. All images were manipulated using Adobe Photoshop CS6 and ImageJ version 2.0.0-rc-65 / 1.52a. No nonlinear modifications were done on the original images. The photos were adjusted in Photoshop to show each plate horizontally and with a size of 2400 x 1800 pixels. Each image was then exported to ImageJ, converted to 8-bit gray scale and inverted. The "ROI" tool was used to measure the colonies to obtain the median, mean and area values. The median gray level values were the averaged for the two colonies from each isolate. These values were fit to a nonlinear regression equation [Agonist] vs. response - Variable slope (four parameters) on GraphPad Prism. Strain H99 was used as an internal control in each experiment. All values were normalized by the value obtained with H99 in the respective experiment.

Laccase activity

Each strain was inoculated into 5 mL YPD (2% glucose, 2% yeast extract) and incubated with 200 rpm agitation at 30°C for 24 hours. The cells were harvested by centrifugation at 1,000 × g for 10 minutes and the culture was resuspended and incubated at 30°C, for 5 days, in 5 mL of asparagine salts medium with glucose (0.3% glucose, 0.1% L-asparagine, 0.05% $MgSO_4$, 1% of solution 1 M (pH6.5) Na_2HPO_4, 3 µM thiamine, 0.001% of solution 0.5 M $CuSO_4$). The cells were harvested by centrifugation at 1,000 × g for 10 minutes and washed once with 5 mL 50 mM Na_2HPO_4 pH 7.0 and washed once with 3 mL asparagine salts medium without glucose. Yeast cells were counted in a hemocytometer and adjusted to achieve an inoculum 10^8 cells/mL. The same number of cells were resuspended in 5 mL of the medium without glucose and incubated at 30°C for 72 hours to induce laccase expression. After incubation, the number of yeast cells per sample were counted in a hemocytometer to normalize the secreted laccase activity in the supernatant by the number of cells

436 present at the end of the culture. The supernatants were harvested at 4,000 g for 5 minutes, and
437 secreted laccase activity was measured in a 96-well plate by adding 180 µL of supernatant from each
438 isolate and 20 µL of 10 mM L-DOPA. To measure laccase activity in whole cells, we prepared
439 suspensions of 10^8 cells/mL of each isolate. In 24-well plates, we placed 450 µL of each isolate
440 suspension plus 50 µl 10 mM L-DOPA. In 96-well plates, we placed 180 µL of the yeast suspension
441 and 20 µl 10 mM L-DOPA. The blank for laccase activity in living cells was 500 and 200 µL cell
442 suspension, respectively. The amount of pigment produced was determined spectrophotometrically at
443 a 480-nm wavelength read every hour for 6 to 48 hours. Absorbance values (OD) converted into
444 laccase activity per yeast with the equation: laccase activity (µmol/number yeast) = mean of OD/(7.9
445 x number yeast at the end of culture). For L-DOPA we used a standard molar extinction coefficient
446 of 7.9 μmol^{-1} (56, 57). Results were reported as the mean of two or three experiments. To adjust for
447 interexperimental variation, laccase activity of the clinical isolates was expressed as a ratio to H99
448 (positive control).

449 **ELISA for GXM quantitation secreted in supernatant**

450 Inocula containing 10^5 cells/mL of each isolate were incubated in 3 mL of minimal medium for 72
451 hours at 30°C under 200 rpm shaking. The cells were precipitated by centrifugation at 4,000 × g for
452 10 minutes, 4ºC and 1.5 mL of the supernatant was transferred to microcentrifuge tubes. Cells debris
453 were precipitated by centrifugation at 15,000 × g for 30 minutes, 4ºC and 1 mL of the supernatant
454 was filtered through a 0.45 µm syringe filter (polycarbonate membrane) and kept at -20 ° C until the
455 time of the ELISA assay. The supernatants were diluted 5,000 and 10,000-fold and analyzed for
456 GXM by enzyme-linked immunosorbent assay (ELISA). A 96-well high binding polystyrene plate
457 (Costar, #25801) was coated for 1 hour at 37ºC with supernatants samples and standard curve of
458 GXM from 0 to 10 µg/mL (H99 GXM standard) and then blocked with 1% bovine serum albumin for
459 1 hour at 37ºC. The plates were then washed three times with a solution of Tris-buffered saline

(0.05%Tween 20 in PBS), followed by the detection of GXM with 50 µL of the monoclonal IgG1 18B7 (1 µg/ml) for 1 hour at 37ºC. The plates were washed three times again and binding of 18B7 was detected with 50 µL of alkaline phosphatase-conjugated GAM IgG1 (Fisher) (1 µg/mL) for 1 hour at 37ºC. The plates were washed three more times and developed with 50 µL of p-nitrophenyl phosphate disodium hexahydrate (Pierce, Rockford) (1 mg/mL). The absorbance was measured at 405 nm after 15 minutes in an EON Microplate Spectrophotometer (Biotek Inc). After subtraction of the blank values, sample measurements were interpolated with a standard four-parameter sigmoidal curve. Values represent the averages of three independent culture and ELISA experiments, performed in different days. The result of each clinical isolate was normalized by the number of cells at the end of the culture time.

Capsule formation

Inocula were made from cultures grown overnight in Sabouraud medium. These cells were grown in 24-well culture plates with four distinct liquid media, with a starting density of 10^6 yeasts/mL. A non-capsule-inducing medium (Sabouraud dextrose - Sab) and three capsule-inducing media (58, 59) were used: minimal medium (MM), ten-fold diluted Sabouraud in 50 mM MOPS (SabMOPS) and CO_2-independent medium (Thermo Fisher Scientific) (CIM) for 24 hours at 37°C. Afterwards, 10 µL of yeasts cells were stained using 1:1 India ink. The slides were photographed in a Zeiss Z1 Axio Observer inverted microscope using a 40X objective (EC Plan Neofluar 40X/0.75 Ph 2; Carl Zeiss GmbH) and an MRm cooled CCD camera (Carl Zeiss GmbH). Images were collected and the capsules measured with the ZEN 2012 software. Capsule thickness measurements were normalized by the value obtained with H99 in each experiment. The expressed results are a mean of three independent experiments performed on different days, with 20 cells measured per experiment.

Analysis of extracellular vesicles (EVs)

EVs were obtained from the culture supernatants of each clinical isolate as previously outlined (32), with modifications. Briefly, fungal cells were cultivated in 40 mL of minimal medium for 3 days at 30°C with shaking. The cultures were then sequentially centrifuged to remove smaller debris, filtered through a 0.8 µm filter and the supernatants ultra-centrifuged (Beckman Coulter optima I-90k, SW28 rotor). The precipitate was resuspended in 2 mL of the remaining culture medium. With 1 mL of EV preparations, the hydrodynamic diameter (intensity) and the polydispersity index were measured by Dynamic Light Scattering (DLS) (ZetaSizer Nano ZS90 (Malvern,UK). Vesicle quantification was performed based on the analysis of sterol in their membranes, using a quantitative fluorimetric Amplex Red sterol assay kit (Invitrogen, catalog number A12216), according to the manufacturer's instructions. All samples were analyzed in duplicate and under the same conditions.

Interaction with macrophages from immunofluorescence microscopy and LC3-associated phagocytosis (LAP)

The J774.16 cell line (J774) was purchased from the American Type Culture Collection (ATCC) to study the interaction of clinical isolates with macrophages. Cells were maintained at 37°C in the presence of 5% CO_2 in Dulbecco's modified Eagle's medium (DMEM) supplemented with 10% heat-inactivated fetal calf serum (FCS) and 1% penicillin–streptomycin (fresh medium) (all from Invitrogen). Cells were used between 10 and 35 passages. J774 cells (2×10^5 cells) were plated in a 13 mm round glass coverslip (previously treated with 5% HCL and heated to 90°C for 10 minutes) placed inside a flat-bottom 24-well tissue culture plate (Kasvi) and allowed to adhere for 24 hours. The cell monolayers were then infected with each IgG1-opsonized (mAb 18B7, 10µg/mL) clinical isolate in a proportion of two fungi per macrophage. The cells were co-incubated for 12 hours and then fixed and permeabilized with methanol at −20°C for 10 minutes. The cells were then incubated with rabbit polyclonal antibody to LC3 (Rabbit IgG anti-LC3-beta, Santa Cruz Biotechnology) followed by a fluorescein-conjugated secondary (Goat anti-Rabbit IgG conjugated Alexa Fluor 488,

Invitrogen). After staining, the coverslips were sealed in ProLong Gold Antifade (Invitrogen). Images were collected on a Zeiss Z1 Axio Observer inverted microscope at 63X (Plan-Apochromatic 63X/1.4 NA, Carl Zeiss GmbH) and an MRm cooled CCD camera (Carl Zeiss GmbH) using the ZEN Blue 2 software. For each isolated, 100 macrophages with internalized *C. neoformans* cells were counted and scored as positive for LAP if at least one of the phagocytosed fungi was in an LC3-positive vacuole.

G. mellonella **median survival time**

G. mellonella larvae were reared in glass jars, at 30 °C in darkness. To maintain the colony, sufficient amounts of an artificial diet were added to the jars at least three times a week. Last instar larvae in the 200 mg weight range were injected in the terminal left proleg with 10^4 yeast cells in ten microliters of PBS containing ampicillin at 400 μg/mL. Twelve individuals were infected per group and the larvae were kept at 37°C after infection. Deaths were counted daily and the experiment was terminated when all individuals in the PBS group molted. Molted individuals in any group were censored from the analysis at the day of their molting. The median survival for each clinical isolate was normalized with that observed for H99 in each experiment.

Negative control (inoculated with PBS) and positive control (inoculated with H99) groups were repeated in each experimental set. Two of the three sets were made with *G. mellonella* larvae that had been fed a cereal-based diet, whereas the third set with 11 clinical isolates were fed beeswax and pollen.

Statistics

Values of p lower than 0.05 were considered significant. Spearman's correlation was used to determine the correlation between *in vitro* phenotypes and *in vivo* patient outcomes. Differences between groups were determined using the two-tailed t-test for normally distributed data. Survival in

530 *G. mellonella* infection studies was obtained by log-rank (Mantel-Cox) test using GraphPad Prism
531 software. Results from *G. mellonella* survival studies and were evaluated with Cox proportional
532 hazards regression using IBM SPSS software.

533 **Study approval**

534 Clinical cryptococcal isolates used in this study were obtained from patients enrolled in a
535 clinical study in Brazil. All trials were approved by the Ethics Committee of Fiocruz, Brazil and by
536 the Research Ethics Committee of - FEPECS/SES-DF, Brazil, number: 882,291 and 942,633.
537 Patients or their legal guardians gave written informed consent, including authorization for the
538 storage and use of their clinical isolates for future research. All patients were monitored and treated
539 free of charge by the Brazilian national health system.

Author contributions

Conceived and designed the experiments: HRS, AMN, PA. Performed the experiments: HRS, SOF, GPOJ, CPR, KMG, EMG. Analyzed the data: HRS, AMN. Supplied funding, assisted in data analysis and oversaw writing of the paper: MSSF, ISP, PA, HCP and AC. Obtaining and tracking clinical isolates and data: WFF, AFC, JLJ, VLPJ, LT and MSL. Wrote the first manuscript draft: HRS and AMN. The manuscript draft was revised and approved by all authors.

Acknowledgements

A.M.N was funded by FAP-DF awards 0193.001048/2015-0193.001561/2017 and the CNPq grant 437484/2018-1. M.S.S.F was supported by FAP-DF/PRONEX award 193.001.533/2016. AC was supported by the National Institutes of Health grants 5R01A1033774, 5R37AI033142, and 5T32A107506, and CTSA grants 1 ULI TR001073-01, 1 TLI 1 TR001072-01, and 1 KL2 TR001071 from the National Center for Advancing Translational Sciences. The authors would like to thank Jhones Dias and Alicia Ombredane for experimental assistance, as well as Emma Camacho and Radamés Cordero for the critical reading of the manuscript.

554 **References**

555 1. Rajasingham R et al. Global burden of disease of HIV-associated cryptococcal meningitis: an
556 updated analysis. *Lancet Infect. Dis.* 2017;17(8):873–881.

557 2. Kwon-Chung KJ et al. The case for adopting the "species complex" nomenclature for the etiologic
558 agents of cryptococcosis. *mSphere* 2017;2(1):1–7.

559 3. Perfect JR et al. Clinical practice guidelines for the management of cryptococcal disease: 2010
560 update by the infectious diseases society of America. *Clin. Infect. Dis.* 2010;50(3):291–322.

561 4. Lin X, Heitman J. The biology of the *Cryptococcus neoformans* species complex. *Annu. Rev.*
562 *Microbiol.* 2006;60(1):69–105.

563 5. Chang YC, Kwon-Chung KJ. Complementation of a capsule-deficient mutation of *Cryptococcus*
564 *neoformans* restores its virulence. *Mol. Cell. Biol.* 1994;14(7):4912–4919.

565 6. Kozubowski L, Lee SC, Heitman J. Signalling pathways in the pathogenesis of *Cryptococcus*.
566 *Cell. Microbiol.* 2009;11(3):370–380.

567 7. McClelland EE, Bernhardt P, Casadevall A. Estimating the relative contributions of virulence
568 factors for pathogenic microbes. *Infect. Immun.* 2006;74(3):1500–1504.

569 8. Zaragoza O. Basic principles of the virulence of *Cryptococcus*. *Virulence* 2019;10(1):490–501.

570 9. Robertson EJ et al. *Cryptococcus neoformans* ex vivo capsule size is associated with intracranial
571 pressure and host immune response in hiv-associated cryptococcal meningitis. *J. Infect. Dis.*
572 2014;209(1):74–82.

573 10. Denham ST et al. Regulated release of cryptococcal polysaccharide drives virulence and

574 suppresses immune cell infiltration into the central nervous system. *Infect. Immun.* 2018;86(3).
575 doi:10.1128/IAI.00662-17

576 11. Nosanchuk JD, Casadevall A. Impact of melanin on microbial virulence and clinical resistance to
577 antimicrobial compounds. *Antimicrob. Agents Chemother.* 2006;50(11):3519–3528.

578 12. Grossman NT, Casadevall A. Physiological differences in *Cryptococcus neoformans* strains *in*
579 *vitro* versus *in vivo* and their effects on antifungal susceptibility. *Antimicrob. Agents Chemother.*
580 2017;61(3):1–33.

581 13. Williamson PR, Wakamatsu K, Ito S. Melanin biosynthesis in *Cryptococcus neoformans*. *J.*
582 *Bacteriol.* 1998;180(6):1570–1572.

583 14. Sabiiti W et al. Efficient phagocytosis and laccase activity affect the outcome of HIV-associated
584 cryptococcosis. *J. Clin. Invest.* 2014;124(5):2000–2008.

585 15. Brilhante RSN et al. An alternative method for the analysis of melanin production in
586 *Cryptococcus neoformans sensu lato* and *Cryptococcus gattii sensu lato*. *Mycoses* 2017;60(10):697–
587 702.

588 16. Huang J et al. Activation of antibacterial autophagy by NADPH oxidases. *Proc. Natl. Acad. Sci.*
589 *U. S. A.* 2009;106(15):6226–6231.

590 17. Akoumianaki T et al. *Aspergillus* cell wall melanin blocks LC3-associated phagocytosis to
591 promote pathogenicity. *Cell Host Microbe* 2016;19(1):79–90.

592 18. Kyrmizi I et al. Calcium sequestration by fungal melanin inhibits calcium-calmodulin signalling
593 to prevent LC3-associated phagocytosis. *Nat. Microbiol.* 2018;3(7):791–803.

594 19. Nicola AM et al. Macrophage autophagy in immunity to *Cryptococcus neoformans* and *Candida*

595 *albicans*. *Infect. Immun.* 2012;80(9):3065–3076.

596 20. Panepinto J et al. Sec6-dependent sorting of fungal extracellular exosomes and laccase of
597 *Cryptococcus neoformans*. *Mol. Microbiol.* 2009;71(5):1165–1176.

598 21. Rodrigues ML, Godinho RMC, Zamith-Miranda D, Nimrichter L. Traveling into outer space:
599 unanswered questions about fungal extracellular vesicles. *PLoS Pathog.* 2015;11(12):1–6.

600 22. Matos Baltazar L et al. Antibody binding alters the characteristics and contents of extracellular
601 vesicles released by *Histoplasma capsulatum*. *mSphere* 2016;1(2):1–17.

602 23. Salas SD, Bennett JE, Kwon-Chung KJ, Perfect JR, Williamson PR. Effect of the laccase gene,
603 CNLAC1, on virulence of *Cryptococcus neoformans*. *J. Exp. Med.* 1996;184(2):377–386.

604 24. Williamson PR. Laccase and melanin in the pathogenesis of *Cryptococcus neoformans*. *Front.*
605 *Biosci.* 1997;2. doi:10.2741/A231

606 25. Casadevall A, Perfect JR. *Cryptococcus neoformans*. Washington, D.C: ASM Press; 1998:

607 26. Rosas AL et al. Isolation and serological analyses of fungal melanins.. *J. Immunol. Methods*
608 2000;244(1–2):69–80.

609 27. Pukkila-Worley R et al. Transcriptional network of multiple capsule and melanin genes governed
610 by the *Cryptococcus neoformans* cyclic AMP cascade. *Eukaryot. Cell* 2005;4(1):190–201.

611 28. Camacho E et al. The structural unit of melanin in the cell wall of the fungal pathogen
612 Cryptococcus neoformans. *J. Biol. Chem.* 2019;294(27):10471–10489.

613 29. Liu L, Tewari RP, Williamson PR. Laccase protects *Cryptococcus neoformans* from antifungal
614 activity of alveolar macrophages. *Infect. Immun.* 1999;67(11):6034–6039.

615 30. Erb-Downward JR, Noggle RM, Williamson PR, Huffnagle GB. The role of laccase in
616 prostaglandin production by *Cryptococcus neoformans*. *Mol. Microbiol.* 2008;68(6):1428–1437.

617 31. Yáñez-Mó M et al. Biological properties of extracellular vesicles and their physiological
618 functions. *J. Extracell. Vesicles* 2015;4(2015):1–60.

619 32. Rodrigues ML et al. Vesicular polysaccharide export in *Cryptococcus neoformans* is a eukaryotic
620 solution to the problem of fungal trans-cell wall transport. *Eukaryot. Cell* 2007;6(1):48–59.

621 33. Nosanchuk JD, Nimrichter L, Casadevall A, Rodrigues ML. A role for vesicular transport of
622 macromolecules across cell walls in fungal pathogenesis. *Commun. Integr. Biol.* 2008;1(1):37–39.

623 34. Alanio A, Desnos-Ollivier M, Dromer F. Dynamics of *Cryptococcus neoformans*-macrophage
624 interactions reveal that fungal background influences outcome during cryptococcal
625 meningoencephalitis in humans. *MBio* 2011;2(4). doi:10.1128/mBio.00158-11

626 35. Bielska E, May RC. What makes *Cryptococcus gattii* a pathogen?. *FEMS Yeast Res.*
627 2015;16(1):1–12.

628 36. Hansakon A, Ngamskulrungroj P, Angkasekwinai P. Contribution of laccase expression to
629 immune response against *Cryptococcus gattii* infection. *Infect. Immun.* [published online ahead of
630 print: December 23, 2019]; doi:10.1128/IAI.00712-19

631 37. Mukaremera L et al. The mouse inhalation model of *Cryptococcus neoformans* infection
632 recapitulates strain virulence in humans and shows that closely related strains can possess differential
633 virulence. *Infect. Immun.* 2019;87(5). doi:10.1128/IAI.00046-19

634 38. Xu L et al. Chemokine and cytokine cascade caused by skewing of the Th1-Th2 balance is
635 associated with high intracranial pressure in HIV-associated cryptococcal meningitis. *Mediators*

636 *Inflamm.* 2019;2019:1–9.

637 39. Samarasinghe H et al. Genetic factors and genotype-environment interactions contribute to
638 variation in melanin production in the fungal pathogen *Cryptococcus neoformans*. *Sci. Rep.*
639 2018;8(1):1–11.

640 40. Lee D et al. Unraveling melanin biosynthesis and signaling networks in *Cryptococcus*
641 *neoformans*. *MBio* 2019;10(5). doi:10.1128/mBio.02267-19

642 41. Cordero RJB, Camacho E, Casadevall A. Melanization in *Cryptococcus neoformans* requires
643 complex regulation. *MBio* 2020;11(1). doi:10.1128/mBio.03313-19

644 42. Butler M, Day A. Fungal melanins: a review. Can J Microbiol. *Can. J. Microbiol.* 2011;44:1115–
645 1136.

646 43. Beardsley J, Sorrell TC, Chen SC-A. Central Nervous System Cryptococcal Infections in Non-
647 HIV Infected Patients.. *J. fungi (Basel, Switzerland)* 2019;5(3). doi:10.3390/jof5030071

648 44. Ngamskulrungroj P et al. The trehalose synthesis pathway is an integral part of the virulence
649 composite for *Cryptococcus gattii*. *Infect. Immun.* 2009;77(10):4584–4596.

650 45. Petzold EW et al. Characterization and regulation of the trehalose synthesis pathway and its
651 importance in the pathogenicity of *Cryptococcus neoformans*. *Infect. Immun.* 2006;74(10):5877–
652 5887.

653 46. Levine B. Eating oneself and uninvited guests: autophagy-related pathways in cellular defense.
654 *Cell* 2005;120:159–162.

655 47. Sanjuan MA et al. Toll-like receptor signalling in macrophages links the autophagy pathway to
656 phagocytosis. *Nature* 2007;450(7173):1253–1257.

657 48. Geng J, Klionsky DJ. The Atg8 and Atg12 ubiquitin-like conjugation systems in
658 macroautophagy. “Protein Modifications: Beyond the Usual Suspects” Review Series. *EMBO Rep.*
659 2008;9(9):859–864.

660 49. Trevijano-Contador N, Zaragoza O. Immune response of *Galleria mellonella* against human
661 fungal pathogens. *J. fungi (Basel, Switzerland)* 2018;5(1). doi:10.3390/jof5010003

662 50. Mylonakis E et al. *Galleria mellonella* as a model system to study *Cryptococcus neoformans*
663 pathogenesis. *Infect. Immun.* 2005;73(7):3842–3850.

664 51. Firacative C, Duan S, Meyer W. *Galleria mellonella* model identifies highly virulent strains
665 among all major molecular types of *Cryptococcus gattii*. *PLoS One* 2014;9(8):e105076.

666 52. Bouklas T, Diago-Navarro E, Wang X, Fenster M, Fries BC. Characterization of the virulence of
667 *Cryptococcus neoformans* strains in an insect model. *Virulence* 2015;6(8):809–813.

668 53. Chen YL, Lehman VN, Lewit Y, Averette AF, Heitman J. Calcineurin governs thermotolerance
669 and virulence of *Cryptococcus gattii*. *G3 Genes, Genomes, Genet.* 2013;3(3):527–539.

670 54. Garcia-Solache MA, Izquierdo-Garcia D, Smith C, Bergman A, Casadevall A. Fungal virulence
671 in a lepidopteran model is an emergent property with deterministic features. *MBio* 2013;4(3).
672 doi:10.1128/mBio.00100-13

673 55. Cunha MM et al. Melanin in *Fonsecaea pedrosoi*: A trap for oxidative radicals. *BMC Microbiol.*
674 2010;10. doi:10.1186/1471-2180-10-80

675 56. Bach CE et al. Measuring phenol oxidase and peroxidase activities with pyrogallol, l-DOPA, and
676 ABTS: Effect of assay conditions and soil type. *Soil Biol. Biochem.* 2013;67:183–191.

677 57. Sinsabaugh RL et al. Soil microbial activity in a *Liquidambar* plantation unresponsive to CO 2-

678 driven increases in primary production. *Appl. Soil Ecol.* 2003;24(3):263–271.

679 58. Zaragoza O, Casadevall A. Experimental modulation of capsule size in *Cryptococcus*

680 *neoformans*. *Biol. Proced. Online* 2004;6(1):10–15.

681 59. Ost KS, O'Meara TR, Huda N, Esher SK, Alspaugh JA. The *Cryptococcus neoformans* alkaline

682 response pathway: identification of a novel Rim pathway activator. *PLoS Genet.* 2015;11(4).

683 doi:10.1371/journal.pgen.1005159

684

685 **Figures and figure legends**

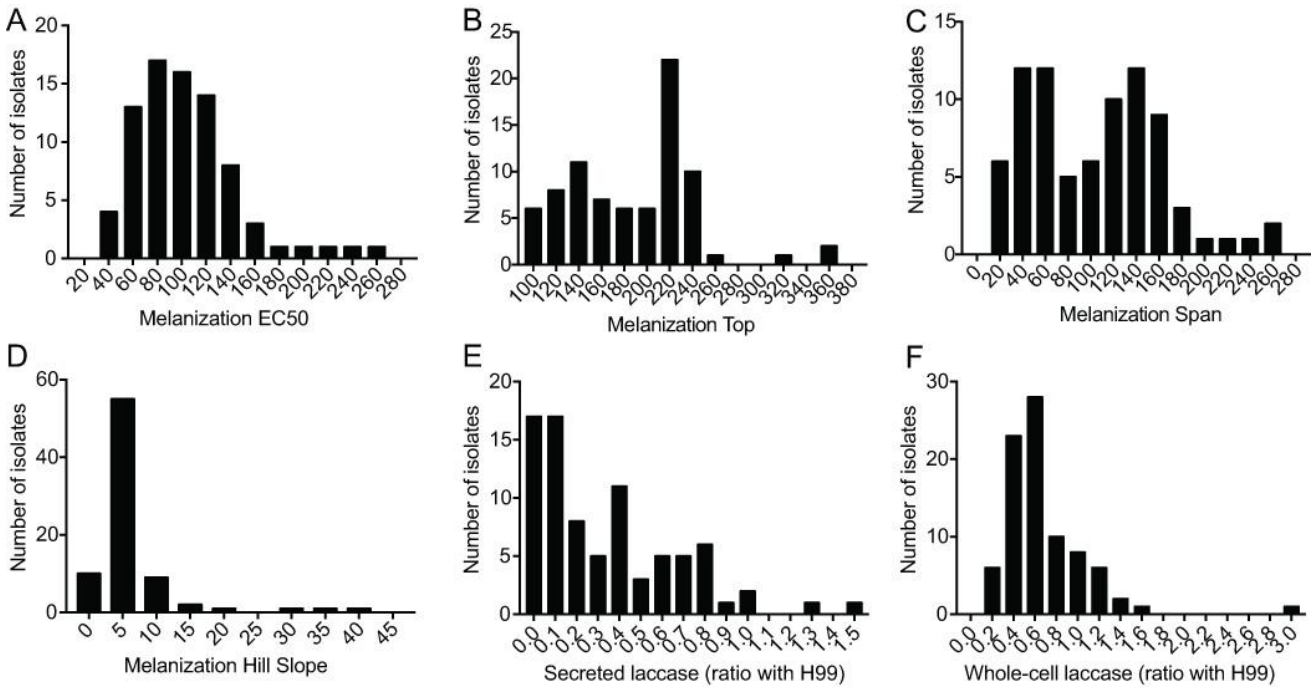

686

687 **Figure 1 – Melanization kinetics of and laccase production by *Cryptococcus* spp. clinical isolates**

688 (A-D) Histograms showing the distribution of the melanization kinetics parameters from clinical
689 isolates. Images of each colony taken throughout 168 h of incubation in melanizing medium were
690 processed and fitted to sigmoidal curves to obtain: (A) melanization EC50 - time in hours for the
691 colony to reach half maximum melanization; (B) melanization Top - median gray level of the colony
692 at the end of the experiment, which indicates how dark the colony became; (C) melanization Span
693 (difference in median gray levels of the colony at the beginning and end of the experiment); (D)
694 melanization Slope (slope of the sigmoidal curve at the inflection point, an expression of how fast the
695 colony melanizes. (E-F) Histograms showing the specific laccase activity from clinical isolates.
696 Frequency distribution of secreted laccase activity, n = 82 and (F) Frequency distribution of whole-
697 cell laccase activity, n = 84.

698

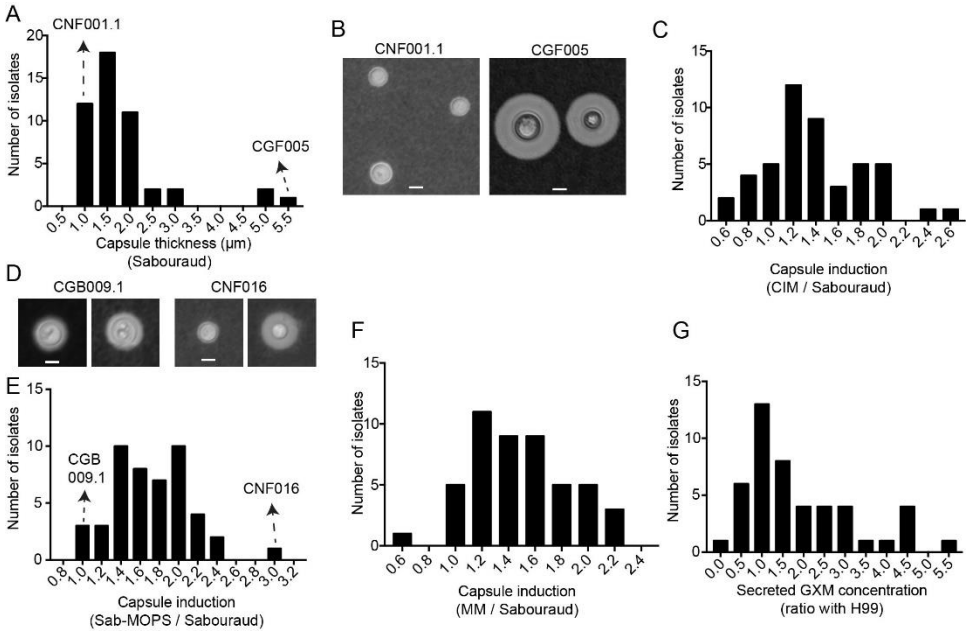

Figure 2 – Capsule size of and GXM secretion by clinical isolates

(A) Frequency distribution of the capsule thickness in Sabouraud medium (Sab), n = 48. (B) Representative photo of isolates at both ends of the capsule thickness distribution, CNF001.1 isolate less than 1 µm thick and CGF005 isolate greater than 5 µm. (C) Frequency distribution of capsule induction in CO_2-independent medium (CIM) relative to Sabouraud (CIM / Sabouraud), n = 47. (D) Representative photo of isolates at both ends of the relative distribution, isolate CGB009.1, which maintained the same capsule thickness in both media, and isolate CNF016, whose capsule was about 3 times larger in Sab-MOPS media (n = 48) and (E) Frequency distribution of capsule induction in Sab-MOPS relative to Sabouraud (Sab-MOPS / Sabouraud). (F) Frequency distribution of capsule induction in Minimum Medium (MM) relative to Sabouraud (MM / Sabouraud), n = 48. (G) Frequency distribution of secreted GXM concentration, n = 46. Experiments were repeated at least twice and had similar results. Scale bars: 5 µm.

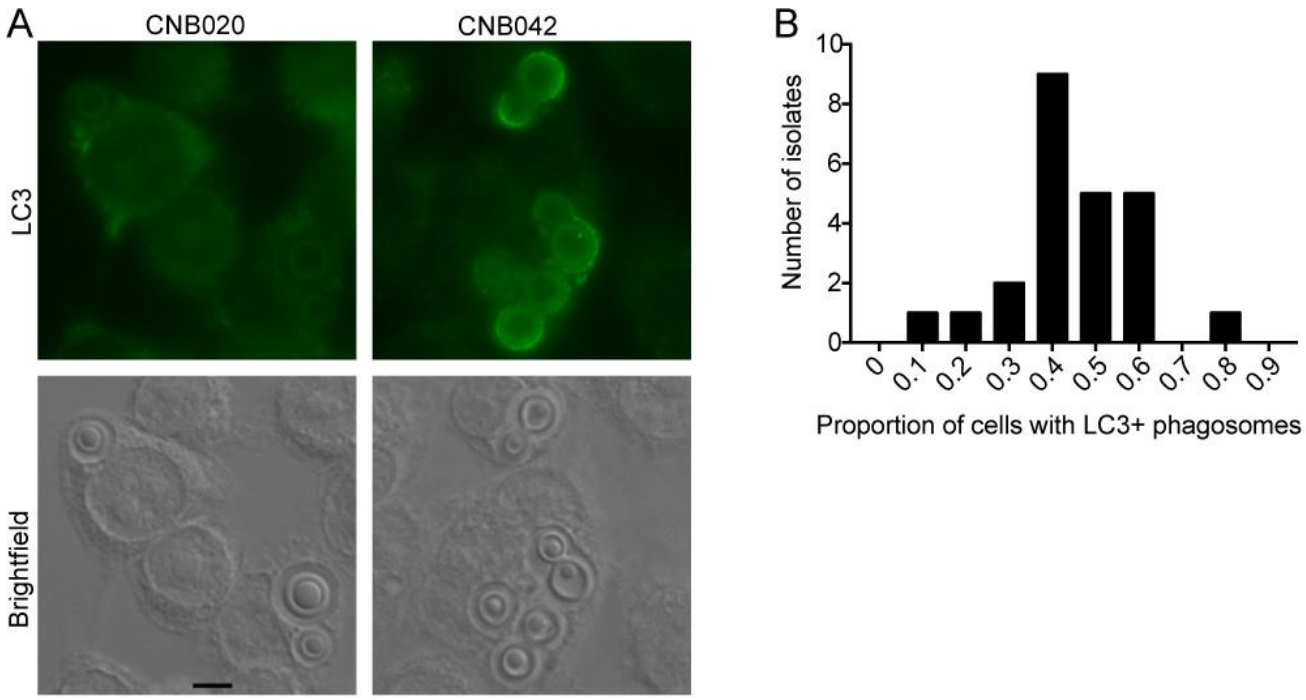

712

713 **Figure 3 – Interaction of clinical isolates with macrophages in LC3-associated phagocytosis**
714 **(LAP)**

715 Representative photo of the autophagy assessment by immunofluorescence, measured by means of
716 phagocytosis associated with LC3 (LAP). Clinical isolate CNB020 with low LAP induction and
717 CNB042 with high LAP induction. (B) Frequency distribution of the proportion of J774 cells with
718 LC3-positive phagosomes, n =24. Experiments were repeated at least twice in different days and had
719 similar results. Scale bars: 10 μm.

720

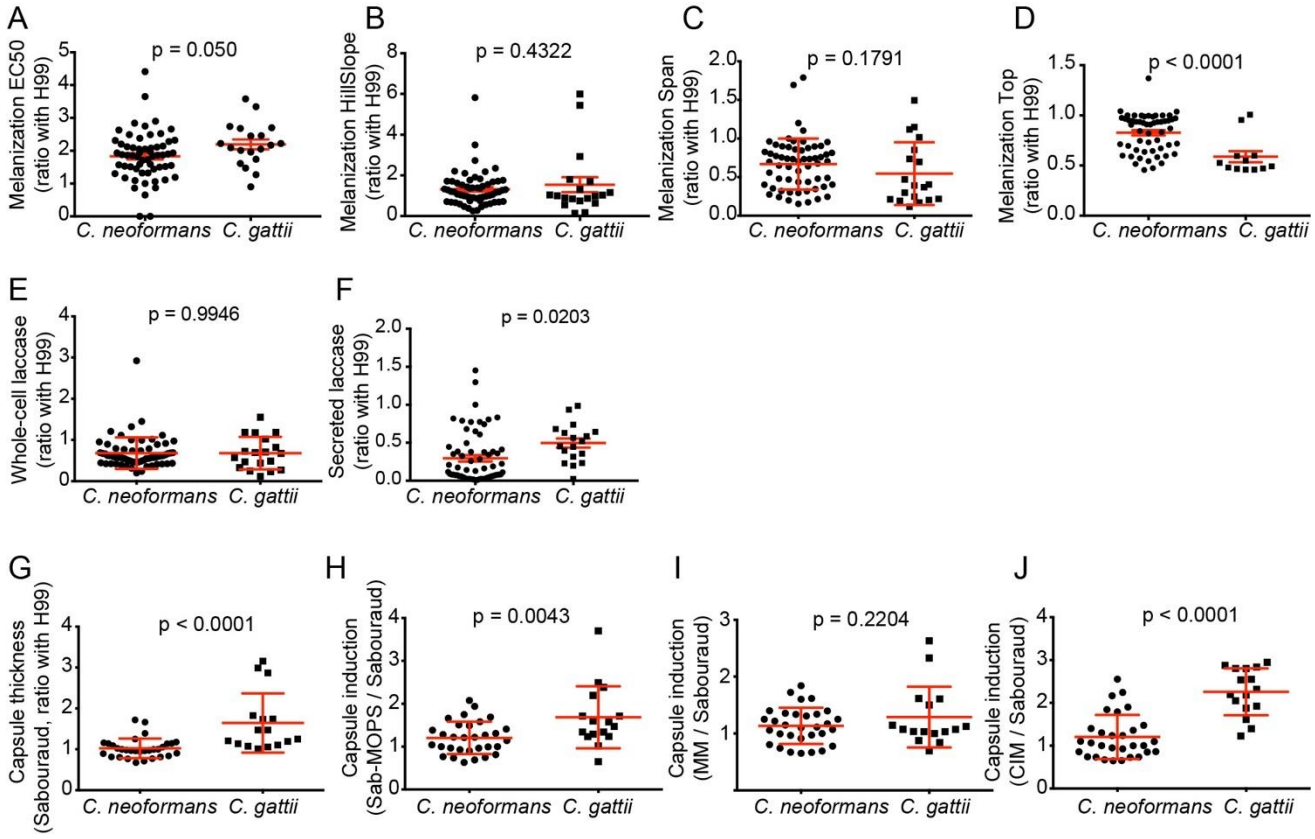

721

722 **Figure 4 – Differences in melanization, laccase production and capsule thickness between *C.***
723 ***neoformans* and *C. gattii* clinical isolates**

724 (A) Differences in melanization EC50 (time in hours for the colony to reach half maximum
725 melanization); melanization HillSlope (slope of the sigmoidal curve at the inflection point,
726 proportional to how fast the colony melanizes); melanization Span (difference in median gray levels
727 of the colony at the beginning and end of the experiment - difference between top and bottom) and
728 melanization Top (median gray level of the colony image at the end of the experiment - proportional
729 to how dark the colony turned), *C. gattii*, n = 19 and *C. neoformans* n = 60. (B) Differences in
730 secreted laccase activity (*C. gattii*, n = 18; *C. neoformans*, n = 64) and whole-cell laccase activity (*C.*
731 *gattii*, n = 19; *C. neoformans*, n = 65). (C) Capsule thickness in Sabouraud medium (Sab) ratio with
732 H99, induction in Sab-MOPS, Minimum Medium (MM) and independent CO_2 relative to Sabouraud
733 (*C. gattii*, n = 16; *C. neoformans*, n = 32). Experiments were repeated at least twice and had similar
734 results. To compare the groups we used two-tailed t-test for independent samples.

735

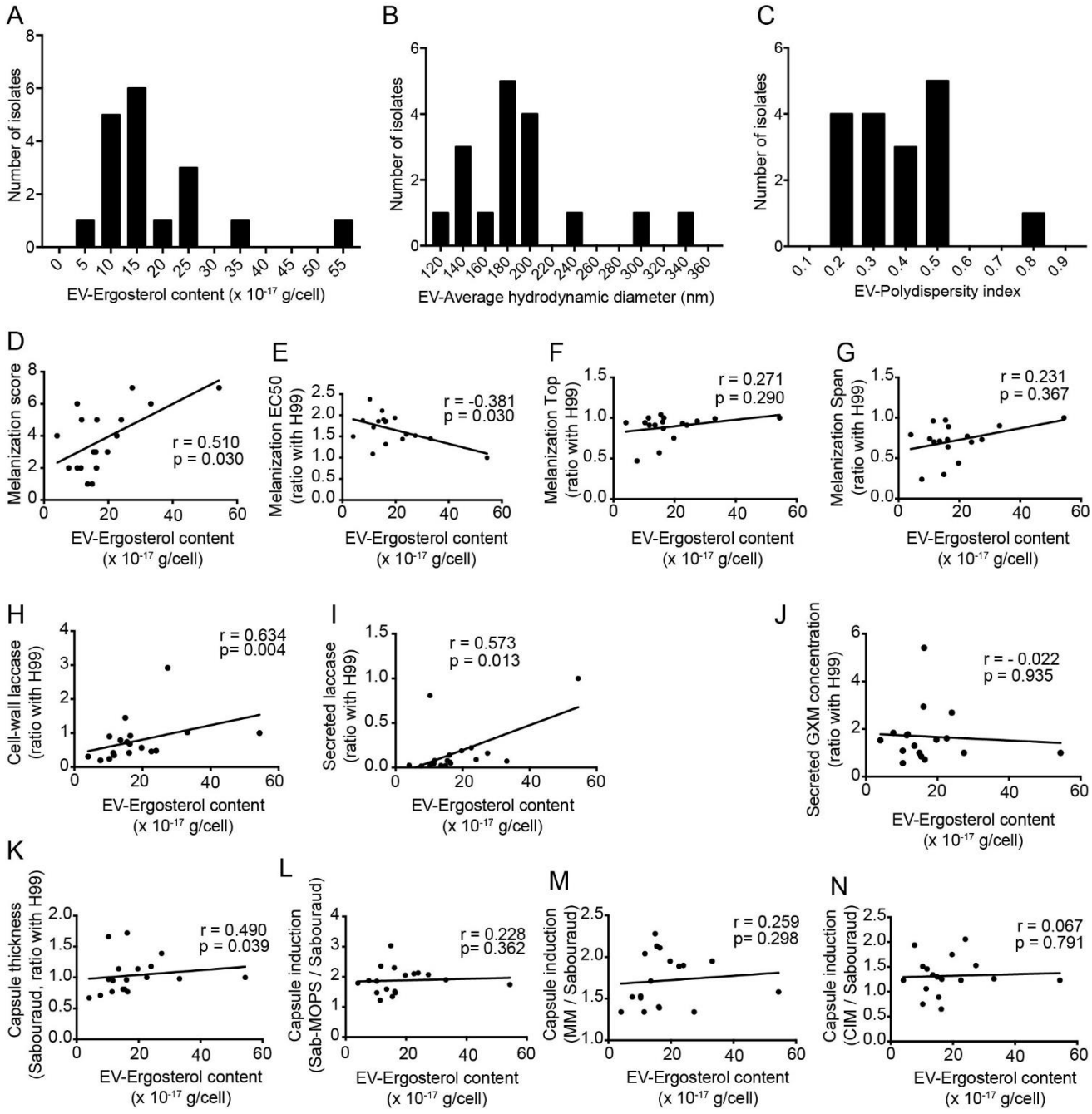

Figure 5 – Extracellular vesicles (EVs) from clinical isolates

EVs preparations were measured by Dynamic Light Scattering (DLS), (A) Frequency distribution of the sterol quantification by sterol amplex red kit (Invitrogen). (B) Frequency distribution of the hydrodynamic diameter (intensity) and (C) Frequency distribution of the polydispersity index. (D) Correlation between EV-Ergosterol content (indicates amount of EV) and classical melanization score (r = 0.634, p = 0.004). (E) Correlation between EV-Ergosterol content and Melanization EC50 (represents the speed of melanization index from non-linear regression curve of median gray value) (r

= -0.381, p = 0.030). (F) No correlation between EV-Ergosterol content with Melanization Top (maximum melanization index from non-linear regression curve of median gray value) (r = 0.271, p = 0.290) or (G) melanization Span (difference in median gray levels of the colony at the beginning and end of the experiment - difference between top and bottom) (r = 0.321, p = 0.004). (H) Correlation between EV-Ergosterol content with cell-wall laccase activity (r = 0.634, p <0.001) and (I) secreted laccase activity (r = 0.573, p = 0.013). (J) No correlation between EV-Ergosterol content and secreted GXM concentration (r = -0.022, p = 0.935). (K) Correlation between EV-Ergosterol content and capsule thickness in medium rich Sabouraud (Sab) (r = 0.490, p = 0.039). (L) No correlation between EV-Ergosterol content with capsule induction in medium Sab-MOPS (r = 0.228, p = 0.362), (M) capsule induction in medium minimal (r = 0.259, p = 0.298) and (N) capsule induction in CO_2-independent medium (r = 0.067, p = 0.791). All samples (n = 18) were analyzed in duplicate and under the same conditions. All correlations were made with Spearman rank.

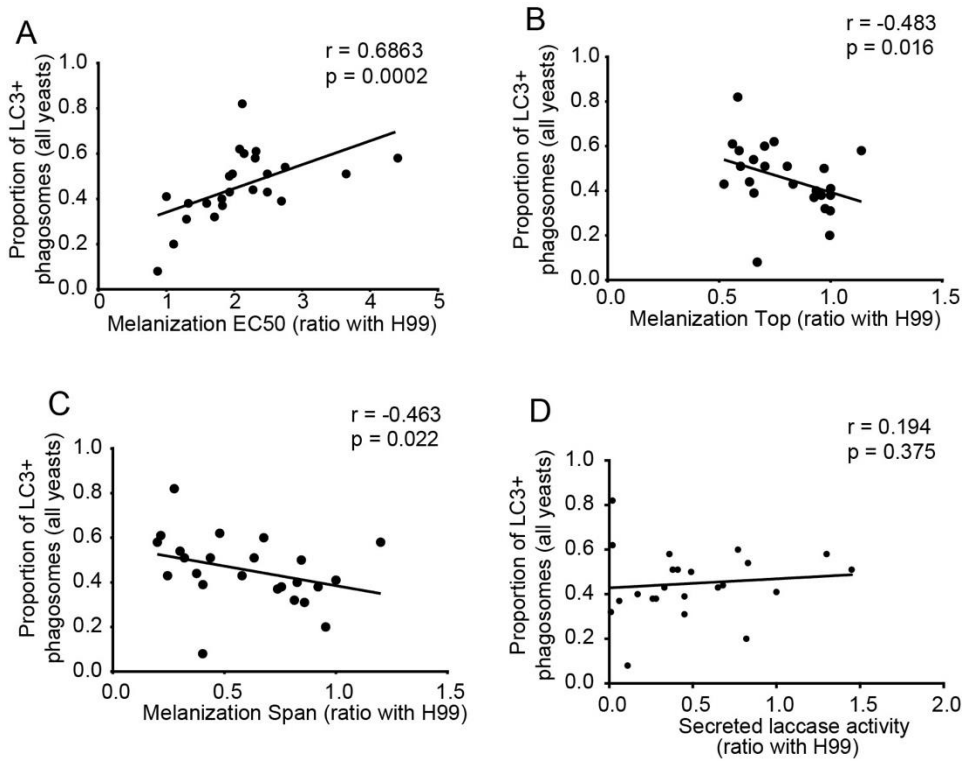

Figure 6 – Melanization kinetics affect the ability of clinical isolates to escape from LC3-associated phagocytosis

Using classical murine macrophages J774, without previous activation stimuli. (A) Correlation between LC3- associated phagocytosis with melanization EC50 (represents the speed of melanization index from non-linear regression curve of median gray value) (r = 0.686, p = 0.0002), (B) with melanization Top (maximum melanization index from non-linear regression curve of median gray value) (r = -0.483, p = 0.016), (C) with melanization Span (difference in median gray levels of the colony at the beginning and end of the experiment - difference between top and bottom) (r = -0.463, p = 0.022) and no correlation with secreted laccase activity (r = 0.194, p = 0.375). All correlations were made with Spearman rank.

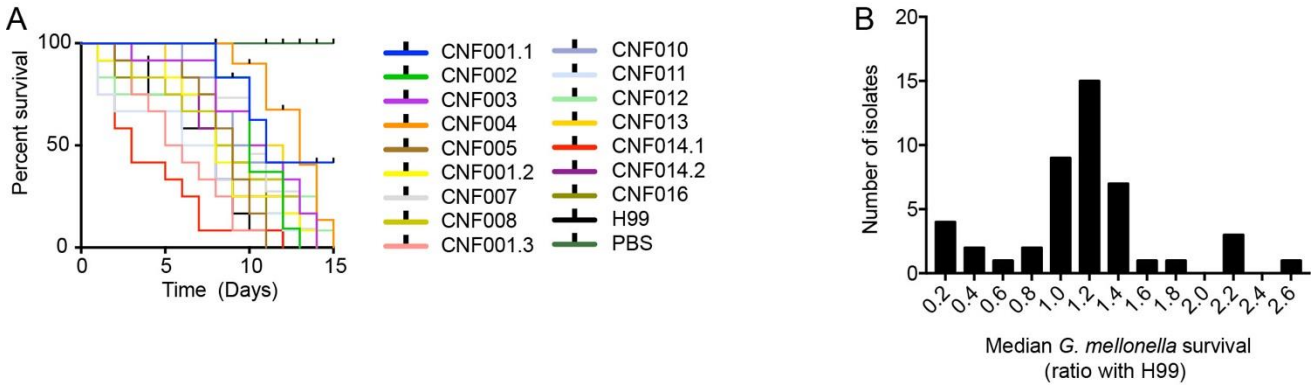

769

770 **Figure 7 - *G. mellonella* survival after infection with different *C. neoformans* isolates**

771 (A) Survival curve of *G. mellonella* infected with clinical isolates. In this experimental batch, all
772 isolates were *C. neoformans* of the molecular type VNI. (B) Frequency distribution of the median
773 survival *G. mellonella* infected with clinical isolates (n = 46). Twelve individuals were infected per
774 isolate.

775
776

Tables

Table 1 – Patient characteristics

Age (years)	42 ± 17.7 (mean ± Std. Dev.)
Gender	68.3% male, 31.7% female
HIV infection status[A]	68.3% positive, 29.3% negative, 2.4% unknown
CD4 count (cells per mm^3)[B]	71 ± 78.9 (median ± Std. Dev.)
Other risk factors[C]	9.8%
Apparently immunocompetent[D]	19.5%
Intracranial hypertension[E]	48.6% - Yes; 10.8% - No; 40.6% - no information
Poor prognosis criteria[F]	58.5%
Two week mortality[G]	30.7%
Ten week mortality[H]	41%

[A]HIV infection determined by serological testing. [B]CD4 cell counts in the peripheral blood of 18 out of 28 HIV-positive patients. [C]Proportion of the 41 patients which had at least one of the following risk factors: diabetes, use of corticosteroids, use of other immunosuppressive drugs or primary immunodeficiencies. [D]Proportion of the 41 patients that were HIV-negative and had no other known immunosuppression. [E]Proportion of the 37 patients with CNS disease that had intracranial hypertension upon the diagnosis of the disease, defined as CSF opening pressure of more than 25 mmHg or papilledema on ophthalmoscopy. [F]Proportion of the patients that had at least one of the following signs or symptoms: confusion, lowered consciousness, coma or focal neurological deficits. [G]Proportion of the 39 patients that were followed for at least two weeks that died before or on the 14th day after the diagnosis. [H]Proportion of the 39 patients that were followed for at least ten weeks that died before or on the 70th day after the diagnosis.

Supplemental data

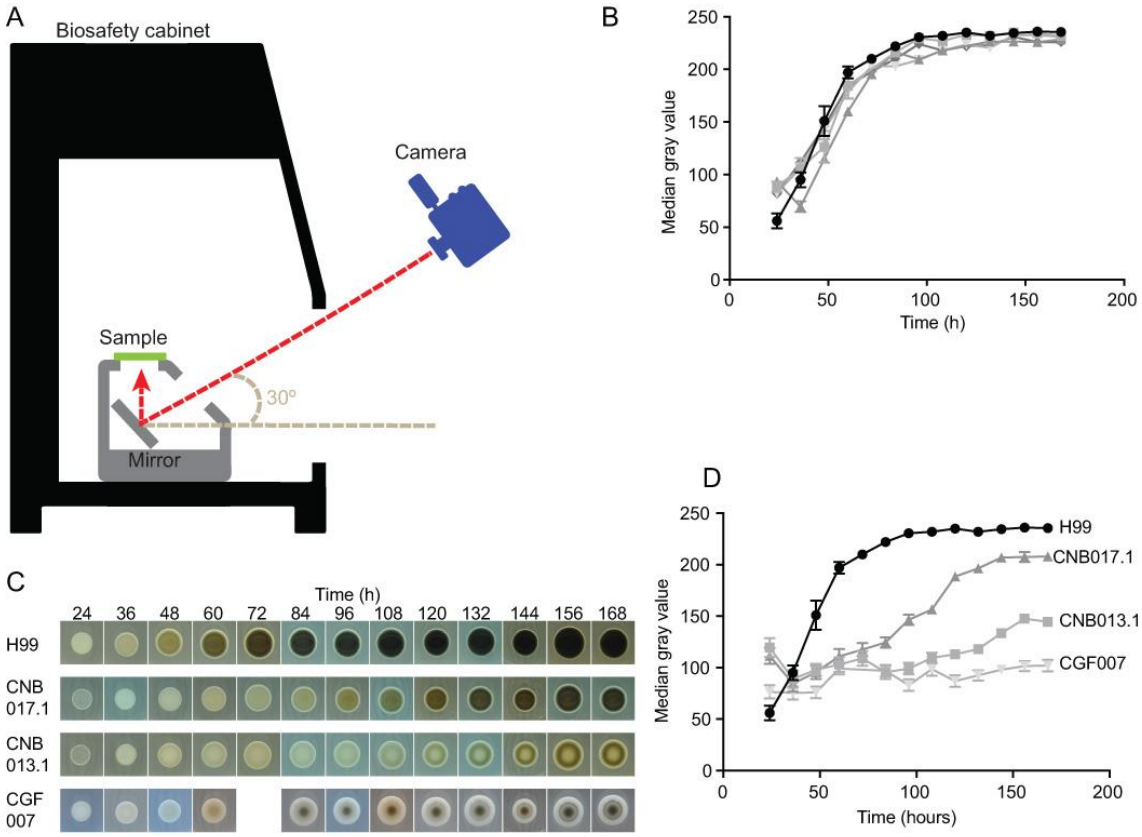

Figure S1

Figure legend. Reproducibility of the new method for quantifying melanin and colony melanization profile. (A) Colony image capture system (mirror plate reflector device developed and manufactured in our research group). (B) Five biological replicates of H99 performed in duplicate technique reveal high reproducibility of the methodology developed to quantify melanin. Three image processing programs were used (Adobe Photoshop CC version 19.0, ImageJ version 1.50i and Prism 7 version 7.0a, respectively) to calculate the median gray values of each colony over time. (C) Representative photo of the macroscopic melanization profile of three clinical isolates and the standard H99 internal control strain in all experiments. Two strains with homogeneous colony melanization (H99 and CNB017.1) and two heterogeneous (CNB013.1 and CGF007). (B and D) Non-linear regression curve of median gray value (represents amount of melanin measured at each observed time).

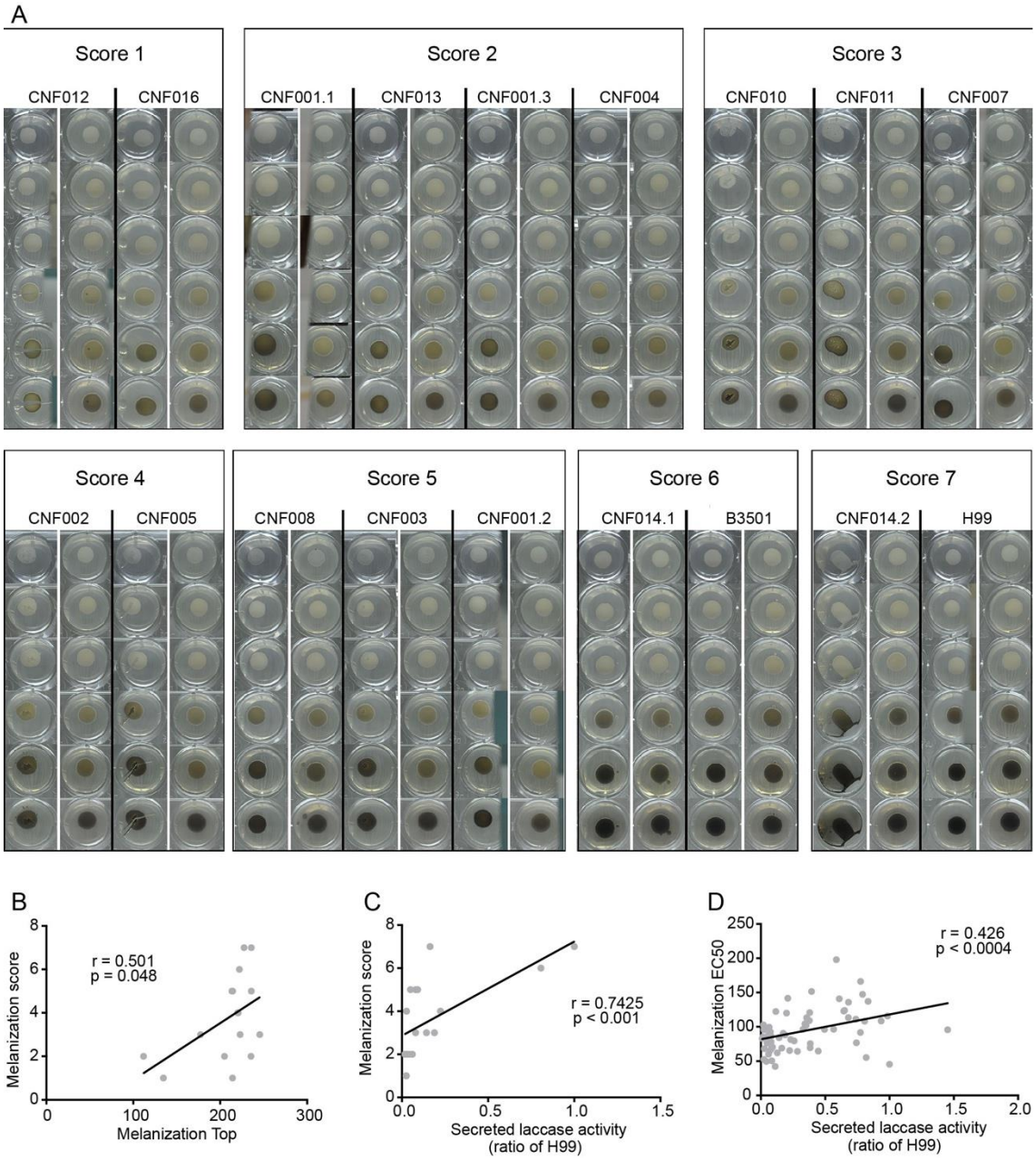

Figure S2

Figure legend. Validation and correlation of the new method for quantifying melanin. (A) Classic semi-quantitative melanization score. The isolates were qualitatively categorized into 7 groups ordered from 1 to 7. Group 1 contains the colony with smaller and later melanization and group 7 the most effective isolates for melanin production. (B) Correlation between Melanization Top (maximum melanization index from non-linear regression curve of median gray value) and classical melanization score ($r = 0.501$, $p = 0.048$). (C) Correlation between secreted laccase activity and classical melanization score ($r = 0.74$, $p < 0.001$). (D) Correlation between secreted laccase activity and Melanization EC50 (represents the speed of melanization index from non-linear regression curve of median gray value) ($r = 0.426$, $p < 0.0004$). Melanization score defined with double blind control of two experienced individuals. All correlations were made with Spearman rank.

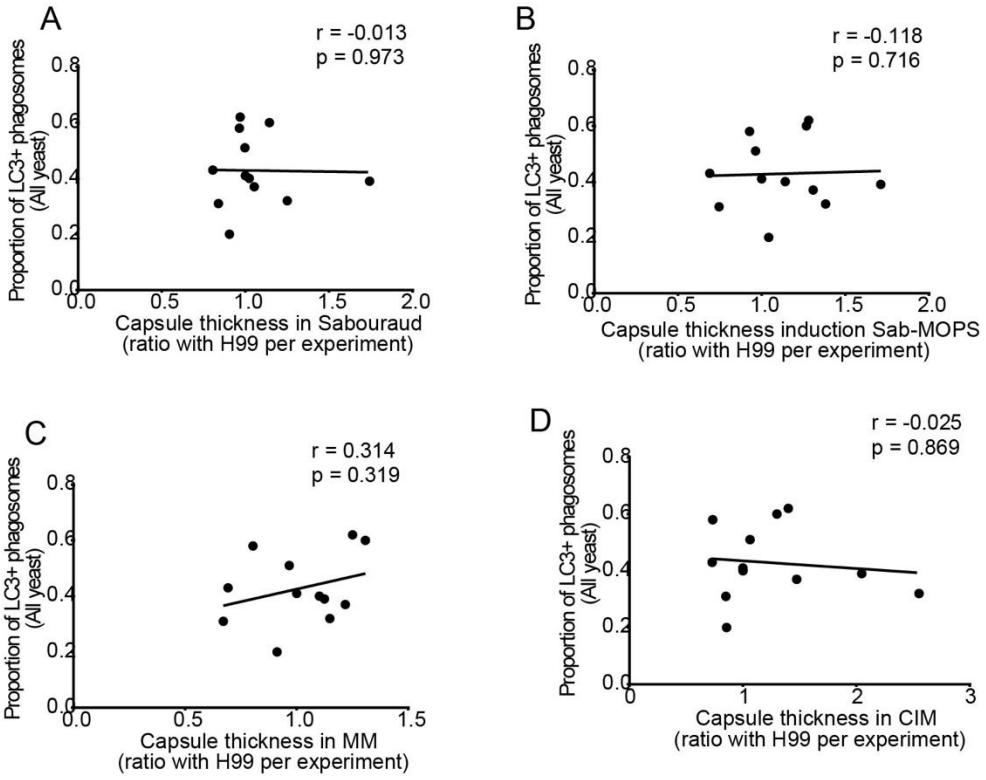

Figure S3

Capsule thickness no affect the ability of clinical isolates to escape from LC3-associated phagocytosis. (A) No correlation between LC3-associated phagocytosis with capsule thickness in medium rich Sabouraud (Sab) (r = -0.013, p = 0.973), (B) with capsule induction in medium Sab-MOPS (r = -0.118, p = 0.716), (C) capsule induction in medium minimal (r = 0.314, p = 0.319) and (D) capsule induction in medium CO_2 independent (r = -0.025, p = 0.869). All correlations were made with Spearman rank.